GAP JUNCTION STRUCTURES

VIII. Membrane Cross-sections

G. E. SOSINSKY,* J. C. JÉSIOR,‡ D. L. D. CASPAR,* AND D. A. GOODENOUGH§
*Rosenstiel Basic Medical Sciences Research Center, Brandeis University, Waltham, Massachusetts 02254; ‡Centere des Études Nucleair Grenoble, Laboratoire de Biologie Structurale/DRF, Grenoble, Cedex, France 38041; and §Department of Anatomy, Harvard Medical School, Boston, Massachusetts 02115

ABSTRACT Profiles of negatively stained gap junctions have been measured by grid sectioning. After normal levels of electron irradiation, the membrane thickness shrinks to about half that of unirradiated controls, but no shrinkage occurs in the hexagonal lattice plane. Even under low irradiation conditions, there is significant thinning of the membranes. Edge views, in which rows of connexons are aligned parallel to the beam, were obtained from grid sections, folds in normal negatively stained specimens, and sections of a positively stained specimen. Averaging these micrographs with the translational and mirror symmetry of the projected lattice image displays conserved and variable features in the stain distribution of different specimens. Variations in the relative amount of negative stain in the gap at the surfaces and in the channel are uncorrelated with the irradiation but appear to depend on the local staining conditions and the integrity of the connexons. The dimensions measured from previously unirradiated grid sections, folds, and positively stained sections are in accord with x-ray diffraction measurements. Radiation-induced shrinkage can be accounted for by mass loss principally from the membrane bilayer. Disordering of the surface structure appears to be correlated with the radiation sensitivity of the bilayer; in contrast, the gap structure is well preserved under a variety of conditions.

INTRODUCTION

Information about the three-dimensional structure of gap junction membranes has been obtained from electron micrographs of tilted specimens (Unwin and Zampighi, 1980; Unwin and Ennis, 1983) and from x-ray diffraction patterns of stacked arrays (Makowski et al., 1982 and 1984). Electron microscopy has revealed variations in the appearance and packing arrangement of the connexon units in the membranes viewed from the surface (Baker et al., 1985), but even with highly tilted specimens, information about the membrane profile is lost in the "missing cone." The grid-sectioning technique (Jésior, 1982*a*) provides a way to visualize the cross-sectional structure of negatively stained membranes.

The connexon units of gap junction membranes form gated channels which regulate intercellular communication (Bennett and Goodenough, 1978; Lowenstein, 1981). Channels through the hexagonally arrayed connexons have been demonstrated in isolated gap junction plaques by electron microscopy (Goodenough, 1976), but the nature of the gating mechanism is not yet clear. Two different gating mechanisms have been proposed: either constriction of the passageway by tilting and twisting of six rigid subunits which form a variable channel (Unwin and Zampighi, 1980), or closing the orifice of a rigid channel by a hinged, six-segmented barrier at the cytoplasmic surface of the connexon (Makowski et al., 1984; Makowski, 1985). More structural data about the movable parts of the connexon are required to explain the gating mechanism.

Labile features identified by comparison of averaged images from micrographs of different negatively stained (Baker et al., 1985) and frozen-hydrated (Sosinsky et al., 1986) specimens may correspond to flexible surface structures. Three-dimensional image reconstructions from negatively stained (Unwin and Zampighi, 1980) and from frozen-hydrated specimens (Unwin and Ennis, 1984) have not, however, resolved the surface structure detected by x-ray diffraction from stacked arrays of hydrated gap junction membranes (Makowski et al., 1982; Makowski, 1985). Micrographs of tilted, negatively stained gap junction membranes were recorded to establish if the labile features of the connexon structure were, in fact, located at the cytoplasmic surface (Sosinsky, G.E., T. S. Baker, D. L. D. Caspar and D. A. Goodenough, unpublished observations). Measurement of the displacement of hexagonal stain features in pairs of micrographs at different tilt angles indicated that, if these features were on opposite cytoplasmic surfaces, then the thickness of the gap junction membrane pair must have shrunk considerably compared with the 160–180 Å thickness measured by x-ray diffraction (Makowski et al., 1984). The three-dimensional reconstructions calculated from tilt series of negatively stained gap junctions by Unwin and Zampighi (1980), in fact, indicated substantial flattening of the membranes.

Direct measurement of the thickness of negatively stained specimens can be made using the grid sectioning technique (Jésior, 1982*b*). The negative stain acts as a fixative and contrasting agent. Lattice dimensions of embedded and sectioned negatively stained crystals measured parallel to the grid surface correspond closely to those measured face-on before embedding. However, the lattice dimension of thin catalase crystals perpendicular to the grid surface, measured after preliminary observation on finder grids to orient the negatively stained crystals for sectioning (Jésior, 1982*b*), is less than half that determined by x-ray diffraction (Unwin, 1975). Berriman and Leonard (1986) have established, from electron diffraction measurements on negatively stained, thin protein crystals, that the decrease in thickness is due principally to radiation-induced mass loss from the protein.

We have used the grid-sectioning technique to measure the effect of irradiation on the thickness of negatively stained gap junction membranes. Comparisons were also made with sections of a positively stained specimen fixed in the hydrated state. Edge views of gap junctions oriented along principal lattice directions have been observed previously from thin sections (Zampighi et al., 1980) and from folds in negatively stained specimens (Goodenough, 1976; Zampighi et al., 1980; Unwin and Zampighi, 1980). By averaging edge views of oriented lattice domains with the symmetry of the projected image, we have characterized variable and conserved features in the stain distribution of different specimens. The results of this study indicate that the surface structure of negatively stained gap junction membranes may be disordered by radiation-induced shrinkage but the gap structure is relatively stable.

MATERIALS AND METHODS

Negatively Stained Specimens

Gap junctions were isolated and purified as previously described (Fallon and Goodenough, 1981; Baker et al., 1985). Rat liver gap junctions were absorbed to carbon or carbon/formvar grids and stained with 1% uranyl acetate. Low-dose images were recorded from this preparation at a specimen dose of 1–5 $e^-/Å^2$ and a magnification of 42,000, using Philips 410 and 420 electron microscopes equipped with low-dose units at the Whitehead Institute, Massachusetts Institute of Technology, and at the Rosenstiel Center. Edge views were observed from fortuitous folds in these negatively stained gap junction plaques.

Grid Sectioning

The methods used to embed and section grids of negatively stained gap junctions followed the procedure outlined by Jésior (1982*a*) with modifications required for finding small membrane plaques in the grid sections. The microtome was calibrated to cut sections of thicknesses 500 ± 50 Å. The precise location of the membrane plaque chosen to be sectioned was measured from high irradiation electron micrographs of the grid square. Latex spheres on the grid surface were used as markers. The circular cross-sections of these spheres established that distortion due to compression by the knife edge was negligible. After sectioning at the chosen orientation and position of the grid square, the sections were examined in the JEOL 100CX microscope at the EMBL Grenoble. This microscope is equipped with a translation-measuring device attached in series to the translation controls (Jésior and Bois, 1984) which was used to find the plaques in the section relative to a grid bar as marker. Sections of a grid examined at low irradiation (1–5 $e^-/Å^2$) were cut at an arbitrary direction, because the low-magnification image used to locate a region rich in membranes did not resolve the connexon lattice. Sections of air-dried and vacuum-dried grids not previously examined in the electron microscope were cut at random, perpendicular to the grid plane. Images were recorded at magnifications of 30,700 and 61,000.

Positively Stained Sections

A mouse liver gap junction preparation was treated with 0.5% deoxycholate and then centrifuged from the detergent solution. The pelleted membranes were fixed in 2% glutaraldehyde and 1% tannic acid in 0.1 M cacolydate buffer, pH 7.4. Pellets were postfixed in 1% osmium tetroxide, stained en bloc with 1% uranyl acetate, dehydrated in ethanol, and embedded in Epon. Sections were stained with lead citrate.

Image Processing

Images were digitized on a P1000 Photoscan microdensitometer (Optronics International, Chelmsford, MA) and displayed on a television raster graphics terminal. Areas of the membrane cross-sections selected for analysis were boxed using the television screen cursors, and the Fourier transforms were computed on a VAX 11/780 minicomputer (Digital Equipment Corp., Maynard, MA). Fourier averaging of the inplane hexagonal areas followed the procedure detailed in Baker et al. (1983, 1985). Edge views were identified as cross-sections with sharply defined profiles. Edge views were processed by adapting the Fourier averaging methods developed for analysis of crystalline lattices. High spatial frequency noise was removed from the processed images by multiplying the transforms by a circular filter mask with a gradual fall-off at 1/20 Å spacing.

Membrane profiles were determined by back-transforming just the meridian of the computed Fourier transform of edge views. The meridian is the Fourier transform of the density projected onto a line perpendicular to the membrane plane. Thus, the back transform is the one-dimensional profile. Positions of the peaks and troughs of the stain distribution across the membranes were measured from the scaled profiles plotted on a Tektronics terminal. In profiles of stacks of gap junction membranes, there is a single peak in the stain distribution at the apposition of cytoplasmic surfaces. Because the average separation of these peaks in profiles of arrays was similar to that between peaks at the cytoplasmic surfaces for single gap junctions, this peak separation was taken as a measure of the membrane pair thickness. The bilayer pair separation was defined as the distance between stain-excluding troughs in the profiles.

To identify cross-sectional views in which the lateral array of connexons was well ordered, we filtered the images by masking the meridional portion of the transform with a Gaussian strip. This procedure removes the image of the laterally averaged profile of the stain distribution, which is often asymmetric on the two sides of the junction. The filtered image, excluding the meridional data, shows the periodicity and symmetry of the connexon arrangement in the gap.

Symmetry Averaging

Viewed along rows of connexons, the projected image of a cross-section of the hexagonal junction lattice will have the translational symmetry of the row spacing, and mirror symmetry about lines perpendicular to the membrane plane. These mirror lines are located along the hexagonal connexon axes and midway between these axes. The noncrystallographic twofold axes relating connexon pairs at the center of the gap generate a mirror line in projection, along the midplane of the gap, which relates the cylindrically symmetric portions of the connexon pairs. Because the effective resolution of the micrographs of gap junction cross-sections is at best ~30 Å, only the cylindrically symmetric components contribute significantly to the connexon pair image. Micrographs of oriented edge views, showing ordered connexon arrays, were averaged with the transla-

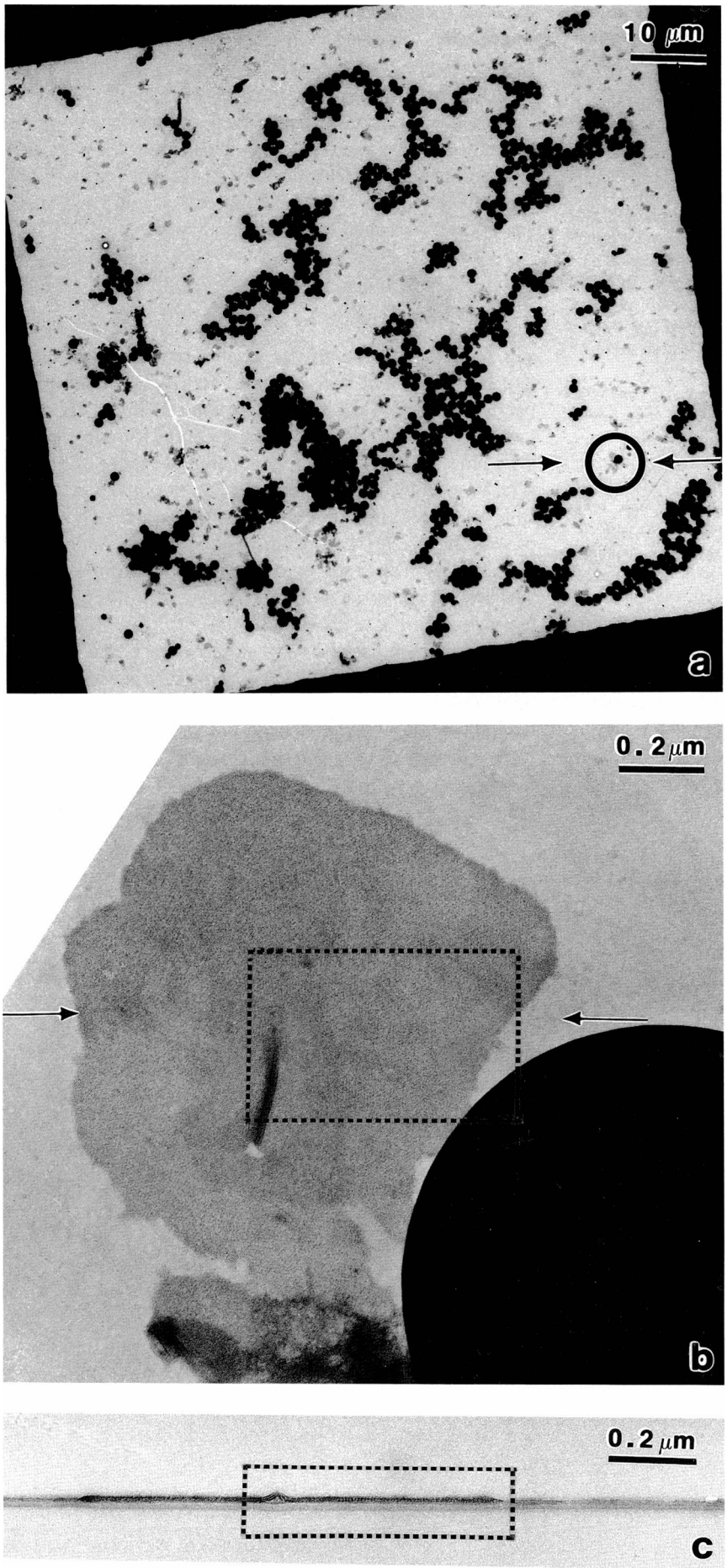

FIGURE 1 Grid sectioning of negatively stained gap junction membranes. (*a*) Low-power micrograph of a grid square with one gap junction plaque and a polystyrene latex sphere circled. (*b*) High-dose, high-magnification micrograph of the membrane plaque and latex sphere circled in *a*. (*c*) Grid section of the membrane in *b*. Note the correspondence between the crease in the membrane seen face-on in *b* and edge-on in *c*. The arrows in *a* and *b* indicate the section plane through the gap junction plaque. The boxed areas in *b* and *c* are shown at higher magnification in Fig. 2.

tional periodicity and with the orthogonal mirror symmetry of the **mm** point group to reduce the contributions of noise, disorder, and noncircularly symmetric portions of the structure to the periodic image. (If higher resolution detail were observed in the micrographs, it would not have been appropriate to average for the mirror line parallel to the gap plane, but the image of the ordered structure would still have the translational periodicity and mirror lines perpendicular to the plane.)

Translational averaging was performed by filtering the computed Fourier transforms for the periodicity of the reciprocal lattice lines corresponding to the connexon row spacing. For local averaging, the lattice lines were masked by a Gaussian strip with a standard deviation width of 1/370 Å. In the filtered image from this mask, the average at any point is weighted for nearest neighbors and includes negligible contributions from units more than five repeats away. For regularly periodic averaging, the lattice lines of the transform were sampled only at the chosen period, which corresponds to averaging equally spaced units all with equal weight.

The origin for the **mm** point group symmetry in the regularly periodic translational average was located by determining the twofold phase origin which minimizes the antisymmetric residual of the transform sampled on the first, second, and third lattice lines. Twofold symmetry was imposed by setting the antisymmetric part of the transform equal to zero, and the **mm** symmetry was then imposed by averaging each lattice line across the equator (or equally, across the meridian). The **mm**-averaged, periodic image was calculated from the symmetry-averaged transform, including the meridional line of data which was centrosymmetrically averaged about the chosen phase origin. The averaged connexon images were displayed with maximum contrast.

RESULTS

Micrographs of cross-sections of embedded, uranyl acetate–stained gap junction membranes suitable for image analysis were obtained from two grids previously examined at high irradiation, one grid examined at low irradiation, and two unirradiated grids, one air dried and the other exposed to high vacuum. Folds in the negatively stained membranes, observed in low irradiation micrographs, also provided some edge views suitable for analysis. A positively stained, fixed specimen, prepared with tannic acid, that had been conventionally embedded and sectioned was also examined. Fourier averages of face views of the negatively stained hexagonal connexon arrays, recorded at both high and low irradiation, were calculated for comparison with the Fourier averaged cross-sectional views.

Grid Sectioning of Negatively Stained Gap Junctions

Fig. 1 illustrates the grid-sectioning technique applied to gap junctions. The membrane chosen for sectioning perpendicular to a [1,0] lattice direction (cf. Fig. 3) is shown circled in Fig. 1 *a* and at higher magnification in Fig. 1 *b*. This junction was chosen for sectioning because of its good size, its well-ordered lattice, and the proximity of a latex sphere used as a marker. The angle between the chosen line of sectioning and the bottom edge of the grid square is 6°. This direction was set by adjustment of the microtome. The section cut at the position of the arrows in Fig. 1, *a* and *b*, is shown in Fig. 1 *c*.

Higher magnification views of the areas boxed in Fig. 1, *b* and *c*, are shown in Fig. 2. The pairs of arrows in Fig. 2 *a* mark the orientation and thickness of the grid section seen edge-on in Fig. 2 *b*. The location of the section in the face view was established using the crease and the edges of the junction plaque as reference. In parts of the grid section (Fig. 2 *b*), periodically spaced dots of stain can be seen in

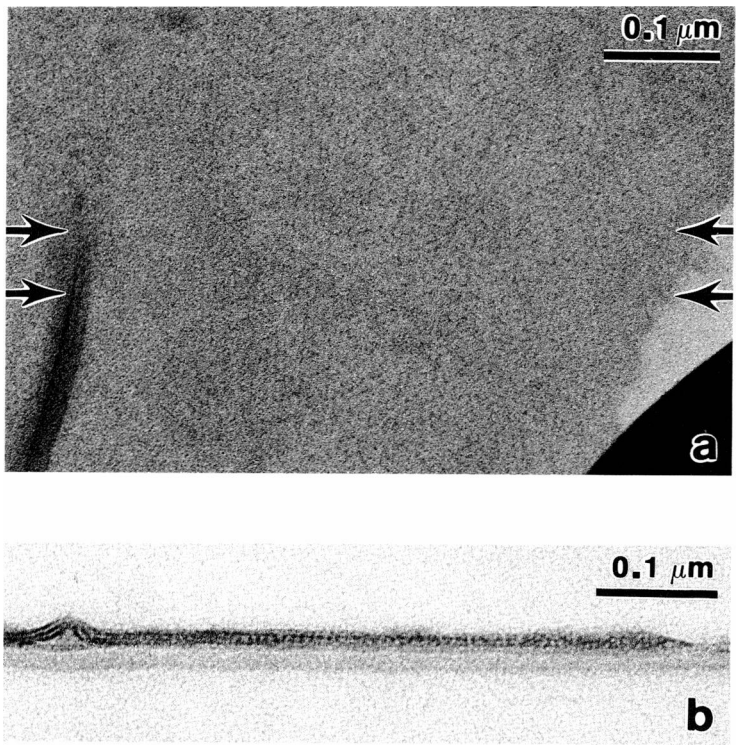

FIGURE 2 Higher magnification views of the boxed areas in Fig. 1. The face view (*a*) shows the hexagonal lattice and the grid section (*b*) shows the concentration of stain in the gap between rows of connexons. The pairs of arrows in *a* mark the orientation and thickness of the section seen edge-on in *b*.

the gap region, corresponding to the projection of the rows of connexons. Blurring of the detail in other portions of this cross-section results from slight tilting of the plane of the membrane and to a small twist of the direction of the lattice rows near the crease and at the right margin.

Fig. 3, which shows Fourier-averaged images of face views of the connexon lattice, illustrates the thickness and orientation of the lattice in the grid sections we have selected for analysis. The sections are 500 ± 50 Å thick; thus, the cross-sectional image of the lattice rows oriented perpendicular to the plane of the section is the projection of six to seven connexons each. In the selected micrographs of grid sections showing regular periodicity in the gap (e.g., Figs. 5 and 6), the rows of connexons are oriented as in Fig. 3. The side-to-side separation of the lattice rows is $\sqrt{3}/2$ times the lattice constant. For the negatively stained specimens, the lattice constant is about 85 Å and the row spacing is, therefore, about 74 Å.

The two images in Fig. 3 compare face views of the lattice from micrographs of the same gap junction preparation recorded at high (Fig. 3 *a*) and low (Fig. 3 *b*) irradiation. Increased irradiation leads to loss of structural detail at the periphery of the connexon. The low-dose, Fourier-averaged image (Fig. 3 *b*) is representative of the detailed images of lattices of skewed connexons obtained in previous studies (Baker et al., 1983 and 1985). The high-dose image in Fig. 3 *a* was averaged from the portion of the gap junction lattice shown in Fig. 2 *a*. This image, unlike most high-dose micrographs of uranyl acetate–stained junctions (Baker et al., 1983 and 1985), shows very little stain, on the average, in the connexon channels. Other high-dose images of the same gap junction preparation show the more typical concentration of stain in the channel. The variability in staining of the channels is also evident in the cross-sectional views (cf. Fig. 5).

Radiation-induced Shrinkage of Gap Junction Thickness

Measurements of the profiles of negatively stained gap junction membranes from grid sections of unirradiated and previously irradiated specimens and from folds in normally viewed specimens, are listed in Table I. Images of flat membrane segments oriented with the membrane plane parallel to the direction of view were selected for measurement. Because the lattice lines are not oriented along the viewing direction in most of these segments, the stain in the gap generally appears as a continuous dark line. Representative edge views and plots of membrane profiles, from images of stacks of two or more gap junctions, are shown in Fig. 4. Table I summarizes the thickness measurements from the profiles of 63 gap junction membrane segments.

Membrane pair thicknesses measured from the distance between stain peaks at the cytoplasmic surfaces for single gap junctions and for stacks from the same type of specimen are not statistically distinguishable. Similarly, the bilayer pair separation, defined as the distance between the stain-excluding troughs in the profiles, appears the same in stacked and individual junctions. Variations in the measurements on comparable specimens, indicated by the standard deviations listed in Table I, are due largely to experimental factors, such as irregularity in stain distribution, which influence the apparent positions of the peaks and troughs of the profiles. These variations are, however, small compared with the systematic decrease in thickness produced by irradiation.

Measurements made on grid sections of specimens that were embedded without previously having been introduced into the electron microscope (e.g., Figs. 4 *c* and 5 *c*), and on folds in the negatively stained specimens imaged at low irradiation (e.g., Figs., 4 *d* and 5 *d*) gave a mean

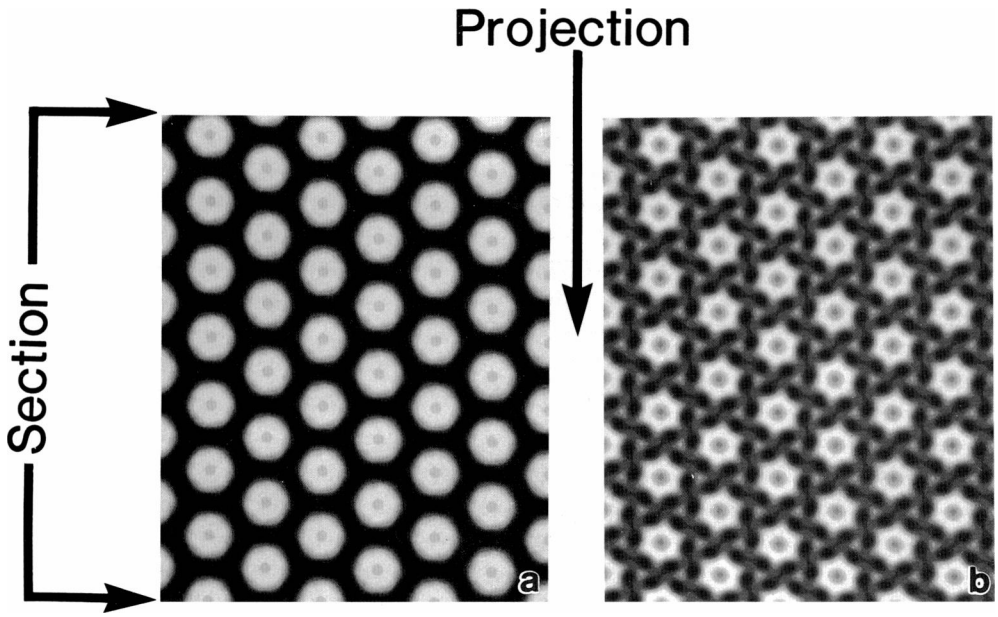

FIGURE 3 Fourier-averaged images of the connexon lattice (*a*) from the portion of the high-irradiation micrograph in Fig. 2 *a*, and (*b*) from a low-irradiation micrograph of another gap junction plaque from the same preparation. Within the accuracy of calibration of the two microscopes used to record these images, the lattice constant is ~85 Å. Sections of grids, in which the lattice is aligned as illustrated here, show the projection of rows consisting of about six or seven connexons each (cf. Figs. 1, 2, 5, and 6).

TABLE I
EFFECT OF IRRADIATION ON THICKNESS OF NEGATIVELY STAINED GAP JUNCTION MEMBRANES

Type of specimen	No. of micrographs	No. of profiles	Mean bilayer pair separation and (STD)	Mean membrane pair thickness and (STD)
			Å	Å
I. Sections				
Preirradiated				
High dose	5	16	45.2 (4.7)	85.3 (5.0)
Low dose	2	8	56.4 (6.4)	110.0 (14.4)
Unirradiated				
Vacuum dried	5	13	—	151.0 (9.2)
Air dried	2	15	75.9 (7.5)	155.0 (10.8)
II. Folds	4	11	76.8 (5.4)	155.1 (6.5)

Mean thicknesses and standard deviations (STD) in Å of negatively stained gap junctions were measured from the density profiles (cf. Fig. 4). High-dose specimens had been exposed to >1,000 $e^-/Å^2$ before embedding and sectioning. Low-dose specimens were exposed to 1–5 $e^-/Å^2$ before grid sectioning. Unirradiated specimens were sectioned from grids which had been vacuum dried or air dried before embedding. Folds in conventionally prepared, negatively stained specimens were imaged under low-dose conditions. Fig. 4 does not include an illustration of a section from an unirradiated grid dried in the electron microscope vacuum before embedding because these sections are similar to Fig. 4 *c* from the air-dried grid. Bilayer separations were not measured for the vacuum-dried specimen because the troughs in many of the density profiles of the edge-on views selected for the thickness measurements were not sharply defined.

membrane pair thickness of 155 Å and a center-to-center bilayer separation of ~76 Å (Table I). The apparent 4 Å decrease in the mean thickness on vacuum drying (Table I) compared with the air-dried specimens is less than the standard deviation of the measurements.

Exposure of the specimen under normal imaging conditions to electron doses >1,000 $e^-/Å^2$ before embedding decreased the measured mean membrane pair thickness to ~45 Å (Table I). The two gap junction membrane cross-sections in Fig. 4 *a* are among the thickest observed after high irradiation, and those shown in Figs. 2 *b* and 5 *a* are close to the average thickness for high irradiation. Exposure to only 1–5 $e^-/Å^2$ under low irradiation condition (e.g., Figs. 4 *b* and 5 *b*) produced about two-thirds the shrinkage observed after high irradiation (Table I).

The bilayer pair separation is about half the membrane pair thickness for all the conditions listed in Table I. Thus, the radiation-induced shrinkage in bilayer pair separation is proportional to the decrease in overall thickness. From comparison of the membrane cross-sections in Figs. 4 and 5, it appears that the thickness of the stain in the gap and at the cytoplasmic surfaces does not change substantially after irradiation. In contrast, the thickness of the stain-excluding layer, corresponding to the position of the lipid bilayer, shrinks significantly even after only low levels of irradiation. Variations in the relative amount of stain in the gap and at the membrane surfaces, which are evident in Figs. 4 and 5, do not appear to be correlated with the conditions of irradiation.

Stain Distribution in Oriented Edge Views

Fig. 5 illustrates the measurement and enhancement of the periodic structure seen in edge views of negatively stained gap junction lattices. The conditions of irradiation of the specimens in Fig. 5 correspond to those shown in Fig. 4: high irradiation cross-section (Fig. 5 *a*); low irradiation cross-section (Fig. 5 *b*); unirradiated cross-section (Fig. 5 *c*); and edge view of a membrane fold (Fig. 5 *d*). Segments of cross-sectional views with evident periodicity (boxed in the panels at the right in Fig. 5) were Fourier transformed (panels at the left in Fig. 5). Transforms of flat segments with extended rows of connexons viewed on edge, such as in Fig. 5 *a*, show well-defined reciprocal lattice lines with a period of ~1/73 Å, corresponding to an 85 Å lattice constant (cf. Fig. 3). In the Fourier transforms of gap junction segments with small-ordered domains, it is sometimes difficult to distinguish the reciprocal lattice lines from the background noise, but the periodicity of the stain concentrations could be measured from the oriented portion of the membrane cross-section. In all the sectioned membranes, the periodicity of the rows of the connexons was 73–74 Å. Thus, irradiation does not alter the lattice constant in the membrane plane, although the thickness decreases by almost a factor of two after high irradiation. The lattice periodicity measured in a short segment of a membrane fold (Fig. 5 d) was slightly larger than that measured in face views (Fig. 3) and in the grid sections (Fig. 5, *a–c*).

Having identified the reciprocal lattice lines corresponding to the periodic rows of connexons in the edge views of oriented lattice domains, the computed Fourier transforms were filtered with a broad lattice line mask and back transformed to locally average the images with the lateral translational symmetry. From the width of the chosen filter mask, the averaging extends over three to four neighboring connexon rows. This averaging procedure reduces the noise in the image without suppressing larger scale variations. The locally averaged images (displayed with enhanced contrast below the images of the membrane segments in each row of Fig. 5) show that the stain in the

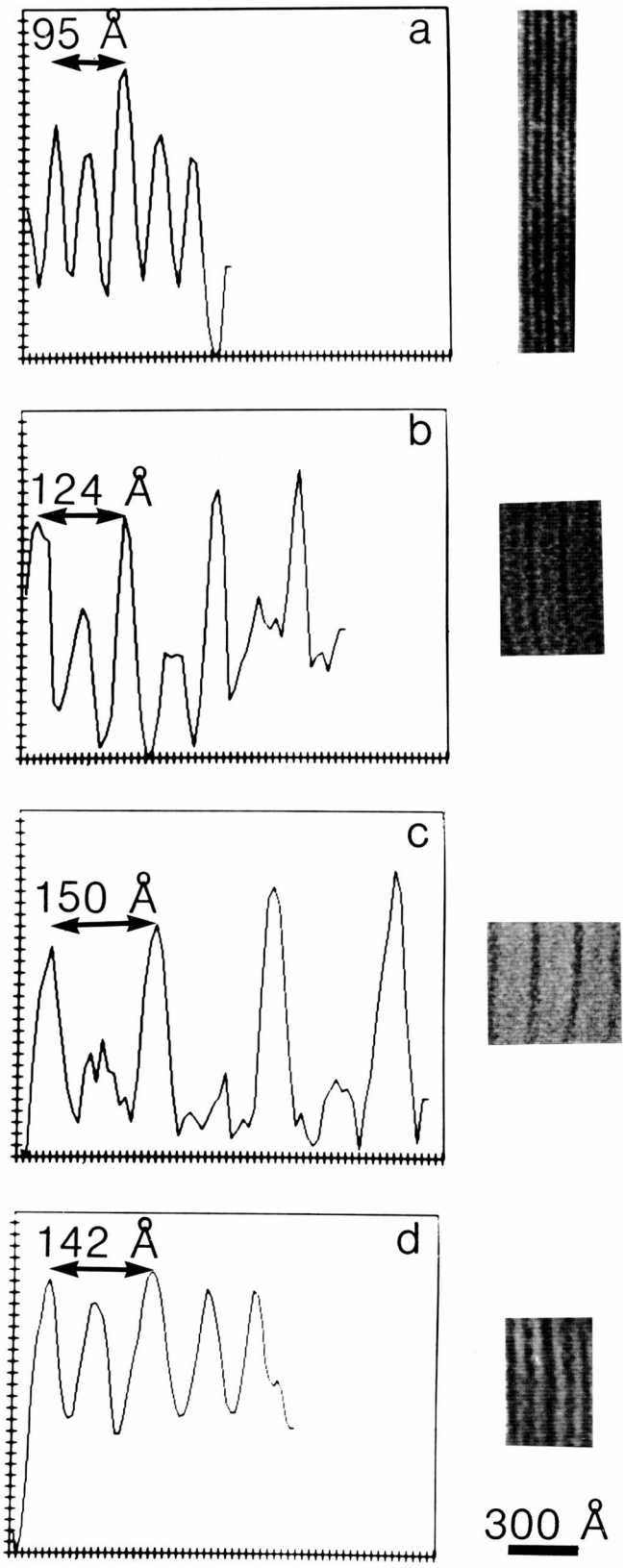

gap appears as well-defined dots when that gap junction lattice is sectioned perpendicular to the rows of connexons (cf. Fig. 3).

The membrane cross-sections in Fig. 5, *a* and *c*, appear asymmetric due to adventitious differences in the amount of stain at the two surfaces, but the stain in the gap displays approximate **mm** symmetry as expected for the low-resolution cross-section of the membrane pair. The most ordered portions of the selected edge views were averaged with the translational periodicity and with **mm** point group symmetry to produce the regular images at the lower right of each row.

Conserved and Variable Features in Averaged Edge Views

Conserved and variable features are evident in the four projected cross-sectional images in Fig. 5 that were averaged with translational and **mm** point group symmetry. Some of the detail may be due to fortuitous superposition of noise in the symmetry averaging, but the major features correlate well with other information about gap junction structures.

Fig. 5 *a*, from a grid exposed to high irradiation, shows no measurable stain, on the average, in the connexon channels but other cross-sections from the same and similar grids show high concentrations of stain in the channels. A moderate amount of stain accumulated in the channels of the low irradiation specimen (Fig. 5 *b*), and axial stain is detectable in the averaged images of the unirradiated specimen (Fig. 5 *c*) and the membrane fold (Fig. 5 *d*). In the averaged face views, more stain is seen at the connexon axis of the low irradiation specimen (Fig. 3 *b*) than in the one exposed to high irradiation (Fig. 3 *a*). Thus, there appears to be no correlation between the axial stain accumulation and the conditions of irradiation. Furthermore, as already noted, the evident variations in the relative amounts of stain in the gap and at the surfaces seen in Figs. 4 and 5 are not correlated with the extent of irradiation.

The rows of stain seen end-on in the gap (Fig. 5) are in the range of 25 to 30 Å thick, but the breadth of these concentrations of stain (which is equal to the row spacing minus the projected diameter of the connexon rows in the gap) appears more variable. The apparent diameter of the averaged connexons in projection is sensitive to small variations in row separation and orientation. Face views

FIGURE 4 Profile plots (*left*) of negative stain distribution in edge views of gap junction segments (*right*). The profiles in *a*, *b*, and *c* are from sectioned grids which, before embedding, had been (*a*) irradiated at high dose, (*b*) irradiated at low dose, and (*c*) not previously irradiated. The profile in (*d*) is from a low irradiation micrograph of a fold in a normally viewed specimen. Arrows mark the distance between a pair of stain peaks at the cytoplasmic surfaces of one junction in each array. Average thicknesses measured from a number of gap junction profiles in each catagory are listed in Table I. Other examples of edge views for the same categories are shown in Fig. 5.

High Dose
Low Dose
Unirradiated
Folds
400 Å
1/73 Å
1/73 Å
1/73 Å
1/77 Å
a
b
c
d
Channel
Gap

(cf. Fig. 3, and Baker et al., 1983 and 1985) show that the mean diameter of the connexon image, which is determined principally by the stain in the gap, is ~60 Å for various staining and irradiation conditions. Thus, the average dimensions and distribution of stain in the gap do not appear to depend on the extent of irradiation or the density of stain. The decrease in thickness of the stain-excluding bilayer with increasing irradiation is clearly evident from comparison of Fig. 5, *a* and *b*, with Fig. 5, *c* and *d*. Some of the images show suggestions of surface projections and indentations which may correspond to the labile surface structure in the negatively stained specimens.

Cross-section of a Positively Stained Fixed Specimen

In the negatively stained specimens, uranyl acetate has acted as fixative, and the specimens have been dried as they were being fixed and stained. To evaluate the possible effects of the dehydration on the membrane cross-section, we examined sections from a specimen that was fixed in the hydrated state and conventionally embedded. The gap junction specimen that was chosen for comparison had been treated with 0.5% deoxycholate, which extracts some of the membrane lipid, producing a more tightly packed connexon lattice (Makowski et al., 1982; Gogol and Unwin, 1986; Tibbitts et al., 1986). The lattice constant for this specimen, measured from the grazing section seen above center in Fig. 6 *a*, is ~80 Å. Tannic acid had been added with the glutaraldehyde fixative, which enhances the binding of the heavy metal ions to the accessible surfaces giving an appearance similar to negative staining. The boxed portion of the darkly stained cross-section in Fig. 6 *a* is oriented with the direction of view exactly along rows of connexons. The high contrast, regular order, and favorable orientation of this portion of the lattice provide a readily analyzable image of the membrane cross-section.

The long-range translational order in the connexon packing and the mirror symmetry of the cross-sectional projection of the boxed segment of the junction membrane (shown at higher magnification in Fig. 6 *c*) are evident in the computed Fourier transform (Fig. 6 *b*). Filtering this transform with the broad lattice line mask produced the locally averaged image shown in Fig. 6 *d*. Further averaging is not necessary to enhance the symmetrical features of the connexon units in this image, because the contrast of the periodic structure is very high compared with the noise level. Clear lines of stain mark the projected rows of connexon channels which are regularly spaced ~70 Å apart.

From the computed membrane profile shown in Fig. 6 *e*, the peak-to-peak separation of the stained surface layers is 177 Å and the troughs of the stain-excluding bilayers are separated by 85 Å. The width of the gap, measured from thickness of the projected rows of stain (Fig. 6 *d*) is 45–50 Å, which is ~20 Å greater than the thickness of negative stain measured in the gap (Fig. 5). Positive staining of the bilayer polar groups can account for this apparent increase in gap thickness.

The greater thickness of the specimen in Fig. 6 compared with those in Figs. 4 and 5 can be attributed to the differences in staining and drying. The overall thickness of the stain-excluding features in the averaged cross-sectional image of the membrane pair (Fig. 6 *d*) is ~180 Å, but some of the wisps of stain-excluding material seen in the unaveraged image (Fig. 6 *c*) extend ~95–100 Å from the center of the gap. In the averaged image, there appear to be two wisps of stain-excluding material at the surface of each connexon unit. It is possible that these surface features are staining artifacts, but the regularity suggests some ordered structure at the cytoplasmic surface.

DISCUSSION

Protein structures are very sensitive to mass loss (Stenn and Bahr, 1970) and disordering (Glaeser, 1971) produced by electron irradiation. In addition, irradiation of negatively stained specimens causes shrinkage and migration of the stain (Unwin, 1974). The radiation-induced shrinkage of gap junction membranes measured from sections of previously irradiated, negatively stained specimens is similar to the dose-dependent shrinkage of thin protein crystals measured from electron diffraction patterns of tilted specimens by Berriman and Leonard (1986). Grid sectioning of

FIGURE 5 Periodic structure in oriented edge views of negatively stained gap junctions averaged by Fourier methods. The micrographs in the upper right panel of each row are from (*a*) a grid section of a single junction, previously irradiated at high dose, with connexon rows aligned along the direction of view; (*b*) a grid section of a stack of junctions, previously irradiated at low dose, with lattice rows in one segment oriented along the direction of view; (*c*) a grid section of a pair of junctions, not previously irradiated, with an oriented segment; and (*d*) a fold in a normally viewed junction with an oriented segment. Fourier transforms, computed from the boxed membrane segments, are shown in the left panel of each row. Lattice lines, shown with amplified intensity in the bottom half of each transform, have been masked by Gaussian strips spaced with the reciprocal of the average periodicity of the stain concentrations (seen in the boxed portion of the corresponding membrane cross-section). The locally averaged images, computed from the filtered transforms, are displayed with enhanced contrast in the center of each row, below the images of the membrane segments. At the lower right of each row is the image averaged with **mm** point group symmetry and regular translational periodicity. These symmetrically averaged images were computed from the most regularly ordered portion of each locally averaged image. All micrographs are shown at the same magnification indicated by the scale bar. The magnification of locally averaged images are 2.5 times and the **mm** symmetry averaged images are 4.5 times that of the micrographs. The positions of the channels and the gap have been marked in the averaged image at the bottom. Variations in the relative densities of stain in the gap, at the surface, and in the connexon channel of different specimens are uncorrelated with the conditions of irradiation. The thickness of stain in the gap, measured from all well-oriented edge views is 25–30 Å, but the thickness of the stain-excluding bilayer, which is 40–45 Å in previously unirradiated membranes (*c* and *d*), decreases to 15–20 Å after high irradiation (*a*).

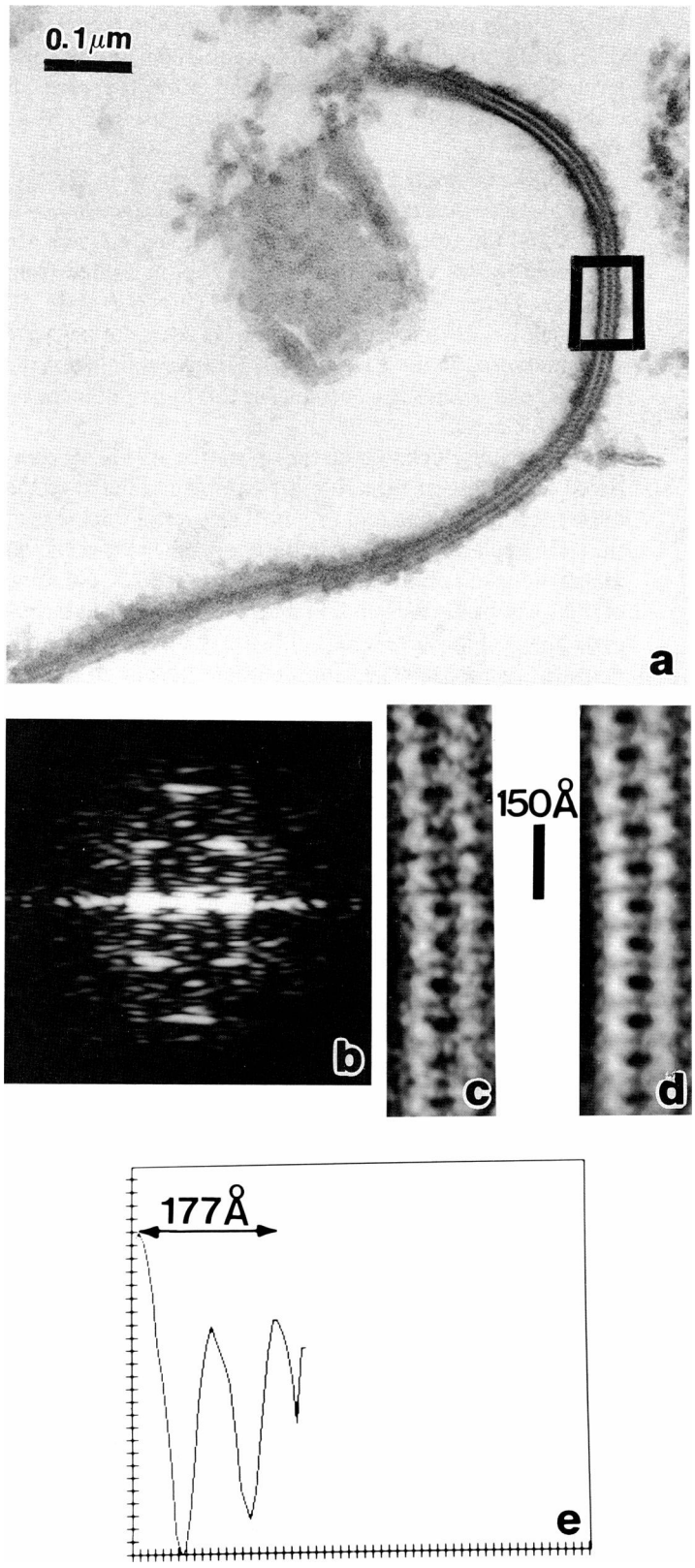

FIGURE 6 Cross-section of a positively stained gap junction. The micrograph in *a* was recorded with high normal irradiation from a deoxycholate-treated specimen that had been fixed in the hydrated state with glutaraldehyde and tannic acid, then postfixed, embedded, sectioned, and stained by conventional procedures. The boxed area of this section shows a well-ordered portion of the lattice which is oriented with the direction of view exactly along rows of connexons. The Fourier transform in *b* was calculated from the boxed segment shown at higher magnification in *c*, with enhanced contrast, after filtering out high spatial frequency noise. The spacing of the reciprocal lattice lines in *b* is ~1/69 Å, corresponding to a hexagonal lattice constant of ~80 Å (as seen face-on in the grazing section, above center in *a*). The locally averaged image in *d* was calculated by filtering the Fourier transform with a broad lattice line mask. The regular periodicity and **mm** symmetry of the projected images of the rows of connexon pairs are clearly evident in *d*. The density profile of this positively stained specimen in *e* has a peak-to-peak separation of 177 Å and an 85 Å separation between the pair of stain-excluding troughs.

irradiated, negatively stained catalase crystals (Jésior, 1982 *b*) had shown that the unit cell dimension perpendicular to the support film was about half that of hydrated crystals measured by x-ray diffraction (Unwin, 1975), but parallel to the grid plane, the lattice dimensions were unchanged.

The results of Berriman and Leonard (1986), correlated with STEM mass loss measurements on unstained proteins (Freeman and Leonard, 1981), establish that most of the shrinkage of negatively stained specimens is due to radiation-induced mass loss from the protein. If the specimen is attached to the support film, the mass loss leads to shrinkage only in the direction perpendicular to the surface, but unsupported portions of the specimen shrink isotropically. The dose-dependent shrinkage is not the same for all specimens. Among the different protein crystals examined by Berriman and Leonard, the dose required to reduce the thickness to one-half that measured with minimal dose (~1 $e^-/Å^2$) ranged from ~10^3 to 10^4 $e^-/Å^2$. For all the specimens, the percentage reduction in the lattice dimension perpendicular to the surface is approximately proportional to the logarithm of the dose over the range measured. Thus, the dose that leads to a 25% decrease in thickness is the square root of that which produces a 50% shrinkage. (Cooling the specimens to liquid nitrogen temperature can prevent the dose-dependent mass loss, but may lead to bubbling if an ice coating forms.) Measurement of the catalase crystal lattice constant perpendicular to the grid at minimal irradiation shows that drying in negative stain leads to a 25–30% shrinkage compared with the native wet crystals. These results of Berriman and Leonard (1986) provide a standard for comparison of our measurements on gap junction membrane thickness from sections of negatively stained grids and conventionally embedded fixed specimens.

Thickness of Negatively Stained Gap Junctions

The data summarized in Table I shows that the thickness of negatively stained gap junction membranes decreased by ~45% after high irradiation and by ~29% after low irradiation, compared with the 151–155 Å thickness measured from sections of previously unirradiated grids and edge views provided by folds in normally viewed specimens. From a previous analysis of the three-dimensional structure of negatively stained gap junctions, Unwin and Zampighi (1980) inferred that the connexon must extend ~75 Å from the central plane, which would produce an overall thickness for the pair of ~150 Å. This conclusion was based on the assumption that the unshrunken membrane thickness should correspond to that measured by Makowski et al. (1977) from x-ray diffraction data. The absolute scale of the two membrane cross-sections plotted by Unwin and Zampighi (1980) was not indicated because, as they noted in the figure caption, the thickness is sensitive to flattening effects which were attributed to the stain drying around the specimen. The position they marked for the approximate location of the cytoplasmic membrane surface in the computed sections is actually ~45 Å from the central plane of the gap (as scaled on the 85 Å lattice constant, which is insensitive to irradition). Thus, their measurements from micrographs of tilted specimens, like our measurements on sectioned specimens, demonstrate that the overall membrane-pair thickness of irradiated, negatively stained gap junctions is <100 Å.

Our results indicate that gap junction membranes are much more sensitive to mass loss in the electron microscope than protein crystals, because irradiation with 1–5 $e^-/Å^2$ produced a shrinkage of the membrane pair by at least 25%, whereas a similar shrinkage of the protein crystals measured by Berriman and Leonard (1986) required 40–90 $e^-/Å^2$. Although a significant decrease in thickness of the gap junction membranes occurred with very little irradiation, further irradiation produced a more gradual shrinkage. Lipid and protein components may have significantly different volatility. Thus, the initial shrinkage may be due to vaporization of some portion of the lipid bilayer, and mass loss from the membrane protein may become significant only at higher doses as for the protein crystals. Quantitative comparison of mass loss from lipid and protein structures by STEM measurements would establish if the postulated differential radiation sensitivity can account for the shrinkage behavior of irradiated gap junction membranes. The decrease in thickness of the stain-excluding membrane bilayer with increasing irradiation is clearly evident from the cross-sectional images in Fig. 5. The connexon protein which spans the membrane does not therefore prevent the collapse which occurs when mass is lost from the bilayer portion.

The 151–155 Å thickness of negatively stained gap junction membranes, measured both from previously unirradiated grid sections and from edge views of folds (Table I), is in good accord with the stacking period of 155–160 Å measured from partially dehydrated centrifuged pellets by x-ray diffraction (Makowski et al., 1977; Tibbitts et al., 1986) and by electron microscopy of sections of these specimens (Caspar et al., 1977). Close packing in the membrane stacks involves some interdigitation or compression of surface protein, because the maximum thickness of the hydrated membrane pair is ~180 Å (Makowski et al., 1984).

Profiles calculated from the meridional x-ray diffraction data show that the bilayer-to-bilayer separation, measured between the electron density minima corresponding to the bilayer centers, is in the range 82–88 Å for both wet and partially dehydrated membrane stacks (Makowski et al., 1977, 1982, 1984). The difference between these x-ray diffraction measurements and the mean separation of ~76 Å, which we have measured between the centers of the stain-excluding layers (Table I), is only slightly greater than the standard deviation of the measurements. This

discrepancy may, therefore, be within the range of the experimental errors. However, x-ray diffraction data indicate that there are solvent accessible pits in the cytoplasmic surface of the membranes (Makowski et al., 1984), and stain concentrations, observed under low irradiation conditions, have been identified with these surface pits (Baker et al., 1985). If some stain can penetrate to the level of the lipid polar groups on the cytoplasmic side but is excluded from the polar layer on the gap side, then the centers of the pair of stain-excluding layers would appear 5–10 Å closer together than the bilayer centers. Our measurements of the profiles of negatively stained gap junctions, which have not been previously irradiated (Table I and Fig. 4) are, therefore, in accord with the surmise that stain can penetrate more deeply on the cytoplasmic than on the gap side of the membranes.

Comparison of Positively and Negatively Stained Cross-sections

The electron micrograph in Fig. 6 *a* provides a clear cross-sectional view of a positively stained gap junction plaque that had been fixed in a fully hydrated state by glutaraldehyde together with tannic acid. Tannic acid acts as a mordant, coating the accessible surfaces of the membrane proteins and binding large quantities of the heavy metal stains to produce a negatively stained appearance. Images of cross-sections from specimens prepared with tannic acid which were obtained by Zampighi et al. (1980) are similar to Fig. 6. The overall thickness of these gap junction membrane pairs measured from the tips of the stain-excluding features at the cytoplasmic surfaces is 180–200 Å. The correspondence between the peak-to-peak separation of the surface stain layers (Fig. 6 *e*) and the mean extent of the stain-excluding features (Fig. 6 *d*) may be fortuitous because the thickness of stain at the surface is variable. The extent and location of the stain-excluding features at the cytoplasmic surfaces are in accord with the x-ray diffraction data (Makowski et al., 1982 and 1984) from fully hydrated specimens.

The overall thickness of the positively stained, tannic acid–treated specimens (Fig. 6; Zampighi et al., 1980) is 20–40 Å greater than that of unirradiated negatively stained specimens (Figs. 4 and 5; Table I). The negatively stained specimens have been either air dried or dried in vacuum before embedding, whereas the positively stained, tannic acid–coated specimens were fixed in the hydrated state before dehydration with alcohol and embedding. The decrease in thickness of the negatively stained, compared with the positively stained, embedded specimens appears to be due principally to the collapse of the projecting fringe of protein at the cytoplasmic surface on air drying. This interpretation is consistent with the x-ray diffraction measurements of the decrease in packing thickness of partially dehydrated membrane stacks (Tibbitts et al., 1986).

The positively stained gap region (Fig. 6) appears ~20 Å wider than the negatively stained gap region (Fig. 5), indicating that positive stain has accumulated in the region of the lipid polar groups on the gap side of the bilayer. The middle of the unstained layer is 40–45 Å from the gap center which coincides with the bilayer position of the native membrane measured by x-ray diffraction (Makowski et al., 1977 and 1982). Thus, the positive staining of the polar layers on the gap and cytoplasmic side must be relatively symmetric. Furthermore, the ~30 Å thickness of the unstained layer corresponds to that of the hydrocarbon core of the native membrane bilayer.

Profiles of gap junctions which have been negatively stained (Fig. 4 and Table I) and positively stained (Fig. 6 *e*) correlate well with the membrane profiles measured by x-ray diffraction, taking into account the probable nature of the stain distributions under different conditions. The dimensions measured in the plane of the thin sections correspond to the dimensions of the specimen when it was embedded, because the radiation-induced mass loss in the plastic embedded sections leads to shrinkage only in the direction perpendicular to the plane (Luther and Crowther, 1984; Taylor et al., 1985), just as for thin specimens attached to a support film (Baker and Amos, 1978; Berriman and Leonard, 1986). Measurements of the thickness of previously irradiated negatively stained specimens by grid sectioning (Table I) therefore provide a reliable estimate of the radiation-induced shrinkage. It would have been very difficult to measure the initial stages of this shrinkage directly from images of tilted specimens because, even at the lowest dose (~1 $e^-/Å^2$) which can produce a measurable image, there is appreciable radiation-induced thinning of the gap junction membranes.

Three-dimensional Structural Information

Alignment of the plane of sectioning perpendicular to a principal lattice direction produces images with interpretable three-dimensional information. The projection of any section contains information about the three-dimensional structure, but without constructive superposition, detail would be lost in the overall noise level. For example, a 1° twist or tilt of the lattice (cf. Fig. 3) relative to the direction of view will displace the two ends of a 500-Å-long row by 9 Å, thus blurring the projected connexon image. Simulations of the blurring produced by tilting the rows of stain (Zampighi et al., 1980) demonstrate how sensitive the sharpness of features in the image is to the orientation. Analysis of the diffraction patterns of grid sections selected for image processing (Fig. 5) indicates that the direction of view is within 1–2° of the principal lattice direction.

By examining the negatively stained specimen on a finder grid (cf. Figs. 1 and 2), the direction of sectioning can be set perpendicular to lattice rows within ~1° (Jésior, 1982*a*), but this requires preirradiation of the specimen.

Because the plane of sectioning can be maintained perpendicular to the grid surface, and the gap junction lattice has sixfold rotational symmetry, the a priori probability that any junction plaque sectioned blind will be within ±1° of the desired orientation is 1/30. The same probability will apply to finding an edge view of a folded junction with similar orientation. However, the probability of finding such an orientation by blind sectioning of an unoriented block is ~1/900. The sharpness of the detail in the boxed portion of the randomly sectioned junction plaque in Fig. 6 indicates that the direction of view is parallel to the lattice rows to within a fraction of a degree and this part of the lattice must be well ordered.

The processed cross-sections of gap junction membranes viewed close to the principal lattice direction (Figs. 5 and 6) illustrate the range of variation of the stain distribution seen in the gap and in the connexon channels. Comparison of Figs. 4 and 5 shows that the relative amount of stain in the gap and on the cytoplasmic surfaces is quite variable. This variation appears to result from fluctuations in the distribution of the stain as the specimen is dried. All of the images selected for processing to illustrate the lattice periodicity (Figs. 5) contain a comparable thickness of stain in the gap. The thickness of the negative stain in the gap is ~30 Å, whether or not the specimens had been preirradiated. The uncertainty in the measurement of this dimension is ~±5 Å, because the exact definition of the boundary depends on how the images have been averaged and on the choice of contrast for the display (Fig. 5). Within the range of the measurements, it appears that the width of stain in the gap changes very little on irradiation compared with the overall shrinkage to about half the initial thickness after high irradiation. Furthermore, the thickness of negative stain in the gap is close to the 30 Å distance between the external bilayer surfaces measured by x-ray diffraction (Makowski et al., 1977, 1982, 1984). The greater thickness of the gap seen in the positively stained junction (Fig. 6) can be attributed to stain accumulation in the polar bilayer surfaces facing the gap.

Definition of the diameter of the gap portion of the connexon seen in cross-sectional projection is not as sharp as that of the gap thickness. The apparent variation in diameter may be due to slight differences in orientation or in the total amount of stain in the gap. Comparison of the averaged face-on views of the connexon lattice image at high and low irradiation (Fig. 3, *a* and *b*) show little difference in the apparent connexon diameter, although the hexagonally symmetric detail is lost or blurred after high irradiation. Thus, the effect of irradiation on the dimensions of the part of the connexon bridging the gap is small compared with the substantial decrease in thickness of the membrane pair. This shrinkage can be attributed principally to the decrease in bilayer thickness due, presumably, to vaporization of lipid components.

The variation observed in the amount of stain in the connexon channel does not correlate with the extent of irradiation (Fig. 5). Previous studies of uranyl acetate–stained junctions (Baker et al., 1983, 1985) comparing different Fourier-averaged face-on images, have shown considerable variation in the amount of stain in the channel. Examination of the unaveraged images shows that some connexons have no stain in the channel and others are densely stained. Irradiation generally enhances the amount of stain seen in the channel, but in our present study some of the high irradiation, uranyl acetate–stained junctions show little stain in the connexon channel from averaged images viewed face-on (Fig. 3 *a*) or in cross-section (Fig. 5 *a*). The small amount of axial staining seen in the face-on average is due to a small number of connexon units which have darkly stained channels. These observations are consistent with the surmise (Baker et al., 1985) that the channels in the isolated gap junction specimens are closed by gates which may become leaky when negatively stained. Radiation damage may enhance the axial accumulation of uranyl acetate stain, but considerable variation in the stain penetration occurs with or without irradiation.

Preservation of Surface Structure

Shrinkage of the gap junction membrane pair normal to the surface by 40 Å or more after irradiation with 1–5 $e^-/Å^2$ (Table I) presents obvious problems in attempting three-dimensional reconstructions from images of tilted specimens. While the low-dose image is being recorded, surface features will be moving. After higher irradiation the thickness may be less variable, but the surface structure is likely to have been disordered by the collapse of the bilayer structure.

X-ray diffraction measurements show that the protein structure on the cytoplasmic surface extends out to ~90 Å from the middle of the gap (Makowski et al., 1982, 1984; Makowski, 1985). Cross-sections of specimens fixed together with tannic acid (Fig. 6; Zampighi et al., 1980) show stain-excluding projections at the cytoplasmic surface which appear to correspond to the cytoplasmic protein domains detected by x-ray diffraction. The fact that this flimsy surface structure has not been observed in freeze-etched specimens (Goodenough, 1975; Hirokawa and Heuser, 1982) may be due to collapse of the unsupported projecting cytoplasmic domains during etching and shadowing. Invisibility of the labile surface structure in three-dimensional reconstructions from negatively stained (Unwin and Zampighi, 1980) and frozen-hydrated specimens (Unwin and Ennis, 1984) may be due to disordering by local surface forces during preparation of the specimen for electron microscopy, as well as disordering from radiation damage. Our observations on cross-sections of gap junction membranes suggest that it may be possible to map the protein structure on the cytoplasmic surface by electron microscopy if well-ordered hydrated specimens can be

suitably fixed and embedded for sectioning perpendicular to different lattice directions, to allow application of three-dimensional image averaging methods.

We thank John Jordan for skillful assistance with specimen purification, Louise Seidel for preparation of the manuscript, Petr Honcu and Judy Black for photography, Linda Melanson for help with sectioning, and Tim Baker for image processing programs and helpful advice.

This work was supported by National Science Foundation grants PCM83-10073 and DMB86-14858, and National Institutes of Health grant CA15468 to D.L.D.C., and National Institutes of Health grant GM18974 to D.A.G. Funds to purchase and maintain the Philips EM420T Transmission Electron Microscope were obtained from a Shared Instrumentation grant S10RR02464-01 awarded to Carolyn Cohen by the National Institutes of Health.

Received for publication 14 October 1987 and in final form 29 December 1987.

REFERENCES

Baker, T. S., and L. A. Amos. 1970. Structure of the tubulin dimer in zinc-induced sheets. *J. Mol. Biol.* 123:89–106.

Baker, T. S., D. L. D. Caspar, C. J. Hollingshead, and D. A. Goodenough. 1983. Gap junction structures. IV. Asymmetric features revealed by low irradiation microscopy. *J. Cell Biol.* 96:204–216.

Baker, T. S., G. E. Sosinsky, D. L. D. Caspar, C. Gall, and D. A. Goodenough. 1985. Gap junction structures. VII. Analysis of connexon images obtained with cationic and anionic negative stains. *J. Mol. Biol.* 184:81–98.

Bennett, M. V. L., and D. A. Goodenough. 1978. Gap junctions, electronic coupling, and intercellular communications. *Neurosci. Res. Program Bull.* 16:375–486.

Berriman, J., and K. R. Leonard. 1986. Methods for specimen thickness determination in electron microscopy. II. Changes in thickness with dose. *Ultramicroscopy.* 19:349–366.

Caspar, D. L. D., D. A. Goodenough, L. Makowski, and W. C. Phillips. 1977. Gap junction structures. I. Correlated electron microscopy and x-ray diffraction. *J. Cell. Biol.* 74:605–628.

Fallon, R. F., and D. A. Goodenough. 1981. Five-hour half-life of mouse liver gap junction protein. *J. Cell Biol.* 90:521–526.

Freeman, R., and K. R. Leonard. 1981. Comparative mass measurement of biological macromolecules by scanning transmission electron microscopy. *J. Microscopy.* 122:275–286.

Glaeser, R. M. 1971. Limitations to significant information in biological electron microscopy as a result of radiation damage. *J. Ultrastruct. Res.* 36:426–482.

Gogol, E., and P. N. T. Unwin. 1986. Gap junction structure: the effects of detergent treatment and lattice variation. *Biophys. J.* 49:204a.

Goodenough, D. A. 1975. Methods for the isolation of mouse hepatocyte gap junctions. *Methods Membr. Biol.* 3:51–80.

Goodenough, D. A. 1976. In vitro formation of gap junction vesicles. *J. Cell Biol.* 68:220–231.

Hirokawa, N., and J. Heuser. 1982. The inside and outside of gap-junction membranes visualized by deep etching. *Cell.* 30:395–406.

Jésior, J. C. 1982*a*. A new approach for the visualization of molecular arrangement in biological microcrystals. *Ultramicroscopy.* 8:379–384.

Jésior, J. C. 1982*b*. The grid sectioning technique: a study of catalase platelets. *EMBO (Eur. Mol. Biol. Organ.) J.* 1:1423–1428.

Jésior, J. C., and J. M. Bois, 1984. Dispositif de repérage micrométrique in situ d'un objet sur une grille de microscope application à l'observation des coupes sériées. *Biol. Cell.* 51:399–402.

Lowenstein, W. R. 1981. Junctional communication: the cell-to-cell membrane channel. *Physiol. Rev.* 61:829–913.

Luther, P. K., and R. A. Crowther. 1984. Three dimensional reconstruction from tilted sections of fish muscle M band. *Nature (Lond.)* 307:566–568.

Makowski, L. 1985. Structural domains in gap junctions: implications for the control of intercellular communication. *In* Gap Junctions. M. V. L. Bennett and D. C. Spray, editors. Cold Spring Harbor Laboratory, Cold Spring Harbor, NY. 5–12.

Makowski, L., D. L. D. Caspar, W. C. Phillips, and D. A. Goodenough. 1977. Gap junction structures. II. Analysis of the x-ray diffraction data. *J. Cell Biol.* 74:629–645.

Makowski, L., D. L. D. Caspar, D. A. Goodenough, and W. C. Phillips. 1982. Gap junction structures. III. The effect of variations in isolation procedures. *Biophys. J.* 37:189–191.

Makowski, L., D. L. D. Caspar, W. C. Phillips, and D. A. Goodenough. 1984. Gap junction structures. V. Structural chemistry inferred from x-ray diffraction measurements on sucrose accessibility and trypsin susceptibility. *J. Mol. Biol.* 174:449–481.

Sosinsky, G., D. L. D. Caspar, T. S. Baker, L. Makowski, S. Maulik, W. Phillips, and D. Goodenough. 1986. Analysis of gap junction electron micrographs based on a three-dimensional model. *Biophys. J.* 49:204a.

Stenn, K., and G. F. Bahr. 1970. Specimen damage caused by the beam of the transmission electron microscope, a correlative reconsideration. *J. Ultrastruct. Res.* 31:526–550.

Taylor, K. A., M. C. Reedy, L. Cordova, and M. K. Reedy. 1986. Image reconstruction using electron micrographs of insect flight muscle. *Biophys. J.* 49:353–364.

Tibbitts, T. T., D. A. Goodenough, W. C. Phillips, and D. L. D. Caspar. 1986. Connexon lattice in gap junctions is compacted by dehydration and lipid extraction. *Biophys. J.* 49:343a.

Unwin, P. N. T. 1974. Electron microscopy of the stacked disk aggregate of tobacco mosaic virus protein. *J. Mol. Biol.* 87:657–670.

Unwin, P. N. T. 1975. Beef liver catalase structure: interpretation of electron micrographs. *J. Mol. Biol.* 98:235–242.

Unwin, P. N. T., and P. D. Ennis. 1984. Two configurations of a channel-forming protein. *Nature (Lond.).* 307:609–613.

Unwin, P. N. T., and G. Zampighi. 1980. Structure of the junction between communicating cells. *Nature (Lond.).* 283:545–549.

Zampighi, G., J. M. Corless, and J. D. Robertson. 1980. On gap junction structure. *J. Cell Biol.* 86:190–198.